

## Vibronic Transitions of Hexagonal Rare-Earth Trichlorides. I. Pr<sup>3+</sup> and Nd<sup>3+</sup> in NdCl<sub>3</sub>\*†

ELISHA COHEN AND H. W. MOOS†

*Department of Physics, The Johns Hopkins University, Baltimore, Maryland*

(Received 12 April 1967)

The absorption spectra of Pr<sup>3+</sup> and Nd<sup>3+</sup> in NdCl<sub>3</sub> have been obtained under high resolution in the 3000–6000 Å region at low temperatures, and under magnetic fields up to 36 kOe. Vibronic transitions are observed accompanying the strong electronic transitions of the rare-earth (RE) ions. The vibronic spectra show a broad, unpolarized absorption band in the phonon-energy region 0–80 cm<sup>-1</sup> which is attributed to acoustical phonons. Many sharp vibronic lines appear in the phonon energy region of 10–270 cm<sup>-1</sup>. These are attributed to optical-phonon branches having **k**'s at various regions of the Brillouin zone (B.Z.). The analysis of these transitions is done by assuming an interaction Hamiltonian between the RE ion and the lattice vibrations which is linear in the phonon normal coordinates. Electric dipole selection rules for single-phonon vibronic transitions are derived for points of high symmetry in the B.Z. The assignment of phonon branches which participate in the vibronic spectrum is made by comparing the polarization of the Zeeman components of the vibronic lines with the set of selection rules. It is found that the sharp polarized vibronic transitions are due to phonon branches which are flat over a wide range of **k**'s along directions of high symmetry in the B.Z. The Zeeman effect of vibronic states is discussed. The energy correction to the energy of the vibronic states is estimated to be less than 1 cm<sup>-1</sup> for both Pr<sup>3+</sup> and Nd<sup>3+</sup>.

### I. INTRODUCTION

THE objectives in the study of vibronic transitions of paramagnetic ions in crystals are twofold: (a) Obtaining information on the interaction between the paramagnetic ion and the dynamic part of the crystalline field. (b) Determining the energies and symmetry properties of the lattice vibrations which contribute to the vibronic spectrum. The rare-earth (RE) ions are especially suitable for such studies as their interaction with the dynamic part of the crystalline field is much smaller than that with the electrostatic field. Consequently, the phonon energies are independent of the electronic states of the RE ion, and on the other hand, the properties of the ion in the electrostatic field are well preserved. Under these conditions it is shown that, to a good approximation, the interaction Hamiltonian is the term which is linear in the phonon normal coordinates,  $V_{ev} = \sum f_{k\Gamma} Q_{k\Gamma}$ . The  $f_{k\Gamma}$  are operators which act on the ionic part only. The spectrum which results from such an interaction displays vibronic transitions involving the creation (or annihilation) of single phonons. The process of a vibronic transition of a RE ion is localized at the ion site, whether it is an impurity ion or a natural constituent of the crystal. Therefore, there are no **k** selection rules and phonons having **k**'s from all regions of the Brillouin zone (B. Z.) participate in the vibronic spectrum. The spectrum reflects, therefore, the structure of the phonon-frequency distribution function, modified by selection rules due to the electronic states and the phonon symmetry.

For these reasons, many attempts were made in the past to interpret observed vibronic spectra. Naturally, simple crystal structures such as alkali halides<sup>1</sup> or

alkaline-earth fluorides<sup>2-5</sup> were chosen in which RE were doped as probes. However, in these cases severe distortion of the vicinity of the RE ion gives rise to local modes. Such complications do not exist in crystals in which the RE ion is a natural constituent or it replaces another RE ion, as is shown in the case studied here. The vibronic spectrum of Pr<sup>3+</sup> in LaCl<sub>3</sub> and LaBr<sub>3</sub> was first studied by Richman *et al.*<sup>6</sup> They analyzed the spectrum by using the vibronics accompanying the transition  ${}^3H_4(\mu \pm 2) \rightarrow {}^3P_0(\mu = 0)$  and assuming contributions from **k**=0 only. Later, Satten<sup>7</sup> suggested that phonons having **k**'s from any region of the B.Z. should be considered and obtained selection rules for points of high symmetry in the B.Z. Loudon<sup>8</sup> discussed the derivation of such selection rules for face-centered cubic, diamond, and zinc-blende lattices and Hobden<sup>5</sup> used them in an attempt to assign phonon branches to observed vibrations in the vibronic spectrum of Eu<sup>2+</sup> in CaF<sub>2</sub>. Weber and Schaufele<sup>9</sup> have observed the vibronic spectrum of Eu<sup>3+</sup> in SrTiO<sub>3</sub> and compared the phonon energies with the phonon branches observed by neutron diffraction.

In the present study an attempt is made to assign phonon branches to observed vibrational levels in the vibronic spectra of Pr<sup>3+</sup> and Nd<sup>3+</sup> in NdCl<sub>3</sub>. Although for this crystal there are 24 phonon branches at a general point **k** in the B.Z., a small number of possible assignments is obtained for each vibrational level. Most of the peaks in the vibronic spectra show polarization in applied magnetic field. However, the components in

<sup>2</sup> D. L. Wood and W. Kaiser, *Phys. Rev.* **126**, 2079 (1962).

<sup>3</sup> J. D. Axe and P. P. Sorokin, *Phys. Rev.* **130**, 945 (1963).

<sup>4</sup> I. Richman, *Phys. Rev.* **133**, A1364 (1964).

<sup>5</sup> M. V. Hobden, *Phys. Letters* **15**, 10 (1965).

<sup>6</sup> I. Richman, R. A. Satten, and E. Y. Wong, *J. Chem. Phys.* **39**, 1833 (1963).

<sup>7</sup> R. A. Satten, *J. Chem. Phys.* **40**, 1200 (1964).

<sup>8</sup> R. Loudon, *Proc. Phys. Soc. (London)* **84**, 379 (1964).

<sup>9</sup> M. J. Weber and R. F. Schaufele, *Phys. Rev.* **138**, A1544 (1965).

\* Partially supported by NASA under Grant No. NSG-361.

† Based in part on a Ph.D. dissertation by E. Cohen, The Johns Hopkins University, 1967 (unpublished). Available through University Microfilms, Ann Arbor, Michigan.

‡ Alfred P. Sloan Foundation Fellow.

<sup>1</sup> W. E. Bron and M. Wagner, *Phys. Rev.* **139**, A232 (1965).

some cases are not completely polarized (as against the electronic transitions which are highly polarized). Thus, these peaks can be attributed to portions of phonon branches which are flat for a large interval of  $k$ 's lying in a direction of high symmetry in the B.Z.

## II. EXPERIMENTAL PROCEDURE AND RESULTS

The absorption spectra of pure  $\text{NdCl}_3$  and 1%  $\text{Pr}^{3+}$  in  $\text{NdCl}_3$  crystals were observed at low temperatures. For wavelength measurements photographic plates were exposed on a 21-ft Paschen spectrograph using a  $4 \times 7$ -in. concave grating with 1200 lines/mm. Intensity measurements were done on a 1-m Jarrell-Ash spectrometer using a  $4 \times 4$ -in. plane grating with 1200 lines/mm. The spectra were taken photoelectrically, in the second order, using an EMI 9558 Q photomultiplier. Most of the data was obtained at 1.4 and 4.2°K, but a few absorption spectra were taken at 77°K. The Zeeman effect of all absorption groups was taken with applied magnetic fields ranging up to 36 kOe.

The crystals used in this work were grown and encapsulated in quartz tubing by E. F. Williams of this laboratory. All samples were single crystals with thickness of 0.1, 2.5, 3.5, and 8 mm. The thin crystals were used for obtaining the positions of the electronic levels and Zeeman splittings while the thicker ones were used for the observation of the vibronic transitions.

The first-order vibronic spectrum of  $\text{NdCl}_3$  spreads up to  $270 \text{ cm}^{-1}$ . Typical spacings between the components of a Stark manifold are of the order of  $10\text{--}50 \text{ cm}^{-1}$ . Therefore, the vibronic spectra associated with the electronic transitions to a given Stark manifold overlap considerably. The only way of determining the correspondence between the vibronic transitions and the parent electronic transitions is by comparing the Zeeman splittings of the two sets of lines. This method was employed for interpreting the structure of vibronic transitions associated with Stark manifolds having  $J \leq 2$  in  $\text{Pr}^{3+}$  and  $J \leq \frac{5}{2}$  for  $\text{Nd}^{3+}$ . For both ions such groups consist of at most 3 Stark components.

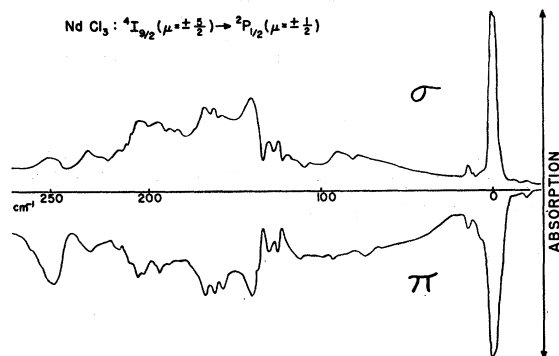


FIG. 1. Photoelectric recording of the absorption transition  ${}^4I_{9/2}(\mu = \pm \frac{5}{2}) \rightarrow {}^2P_{1/2}(\mu = \pm \frac{1}{2})$  in  $\text{NdCl}_3$ . Temperature is 1.5°K and slit width is equivalent to  $0.25 \text{ cm}^{-1}$ . Phonon energies are given above the electronic transition (at  $23193.2 \text{ cm}^{-1}$ ).

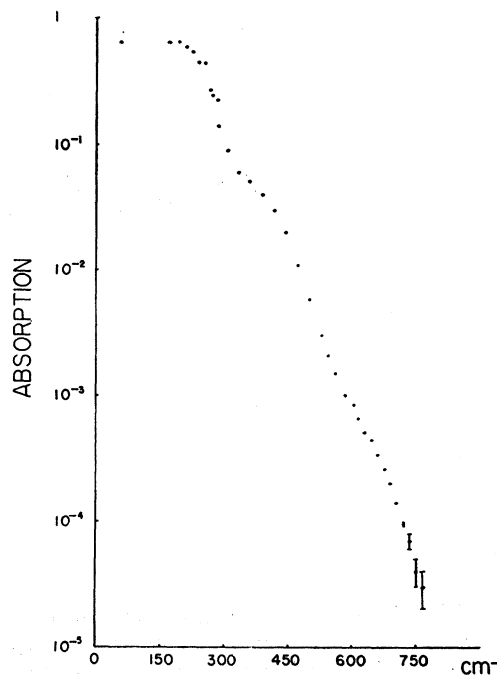


FIG. 2. Intensity of vibronic transitions (on a logarithmic scale) accompanying the transitions  ${}^4I_{9/2}(\mu = \pm \frac{5}{2}) \rightarrow {}^4F_{3/2}(\mu = \pm \frac{3}{2}, \frac{5}{2})$  of  $\text{NdCl}_3$ , and involving the creation of one, two and three phonons. The transitions were observed in the excitation spectrum  ${}^4F_{3/2}(\mu = \pm \frac{1}{2}) \rightarrow {}^4I_{11/2}$  at 4.2°K.

The  $\text{Nd}^{3+}$  ground state ( ${}^4I_{9/2}, \mu = \pm \frac{5}{2}$ ) has a parallel splitting factor<sup>10</sup>  $g_{||} = -4.4$ . At temperatures below 4.2°K and magnetic fields above 15 kOe, absorption vibronic transitions were observed originating at the lower Zeeman component ( $\mu = +\frac{5}{2}$ ) only. The splitting factor of the  $\text{Pr}^{3+}$  ground state ( ${}^3H_4, \mu = \pm 2$ ) is  $g_{||} = 0.8$ . Thus, even at 1.4°K and high magnetic fields there was still an appreciable vibronic absorption from both Zeeman components of the ground state. This fact is important in examining polarization behavior of the vibronic transitions.

The general features of the vibronic spectra of the  $\text{Nd}^{3+}$  ion can be seen in Fig. 1. The parent electronic transition is unpolarized (in zero magnetic field) and so are most of the vibronic transitions. The peak intensity of the vibronic bands is estimated to be at least 100 times smaller than the peak intensity of the electronic transition. The peak intensities of the sharp vibronic lines are of the same order of magnitude. The vibronic spectrum consists of several broad absorption bands on which the sharp peaks are superimposed. In spite of the large continuous absorption, these peaks appeared sharp enough on the photographic plates, enabling the Zeeman effect to be taken. In order to bring up the weak vibronic lines, prints were taken on a high-contrast paper.

The first-order vibronic spectrum cuts off sharply at  $270 \text{ cm}^{-1}$ . Figure 2 shows an excitation spectrum of

<sup>10</sup> G. A. Prinz, Phys. Rev. **152**, 474 (1966).

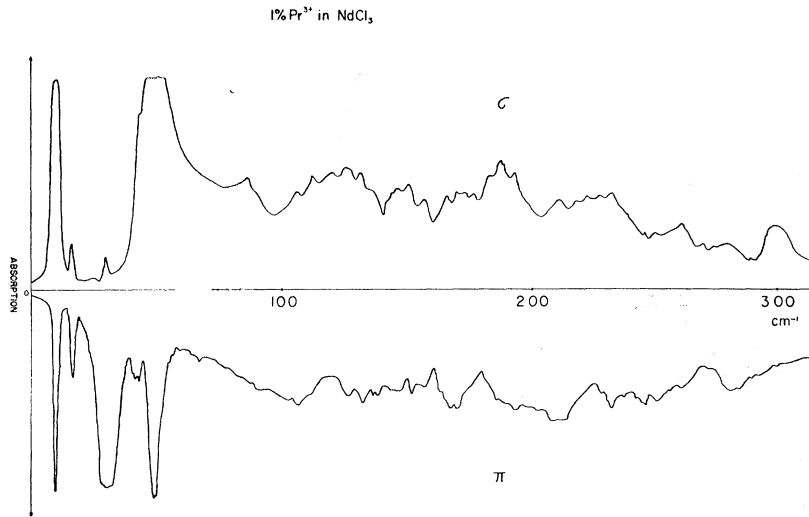


FIG. 3. Photoelectric recording of the absorption transition  ${}^3H_4(\mu=\pm 2) \rightarrow {}^3P_2(\mu=0, \pm 1, \pm 2)$  of  $\text{Pr}^{3+}$  in  $\text{NdCl}_3$ . Temperature is 1.5°K and slit width is equivalent to 0.25  $\text{cm}^{-1}$ . Phonon energies are given above the electronic transition to  $\mu=0$  (at 22168.0  $\text{cm}^{-1}$ ). The other two electronic transitions are at: ( $\mu=\pm 1$ ) 22188.6  $\text{cm}^{-1}$  and ( $\mu=\pm 2$ ) 22208.6  $\text{cm}^{-1}$ .

the transition  ${}^4F_{3/2}(\mu=\pm \frac{1}{2}) \rightarrow {}^4I_{11/2}$  taken with a low-resolution monochromator.<sup>11</sup> The observed absorption is due to vibronic transitions accompanying the electronic transitions  ${}^4I_{9/2}(\mu=\pm \frac{5}{2}) \rightarrow {}^4F_{3/2}(\mu=\pm \frac{1}{2}, \pm \frac{3}{2})$  and involving one, two, and three phonons. The intensity of the second-order vibronic transitions is two orders of magnitude smaller than that of the first-order vibronic spectrum.

Figure 3 shows the vibronic transitions associated with the transition  ${}^3H_4(\mu=\pm 2)$  to  ${}^3P_2(\mu=0, \pm 1, \pm 2)$ . In this case the spectrum consists of the overlapped spectra contributed by each of the electronic Stark components. The vibronic lines show a higher degree of polarization than shown by the  $\text{Nd}^{3+}$  vibronics. As in the case of  $\text{Nd}^{3+}$  vibronics the sharp vibronic peaks are superimposed on broad unpolarized bands and the spectrum cuts off at 270  $\text{cm}^{-1}$ .

The experimental results are summarized in Tables I and II. The phonon frequency is given for each vibronic transition. Also, the polarization of the line (or its Zeeman components), the estimated intensity, and the slope of the magnetic energy versus magnetic field (applied parallel to the  $c$  axis) are given.

### III. THEORY

#### a. General

The system under consideration consists of a single  $\text{RE}^{3+}$  imbedded in the crystal and the set of lattice vibrations. The Hamiltonian for this system has the form

$$H = H_{\text{el}} + H_{\text{vib}} + V_{\text{ev}}. \quad (1)$$

<sup>11</sup> We wish to thank W. B. Gandrud for performing this measurement.

$H_{\text{el}}$  is the Hamiltonian of the RE ion in the electrostatic crystalline field which is produced by the rest of the ions situated at their equilibrium positions:

$$H_{\text{el}} = H_{\text{free ion}} + V_0. \quad (2)$$

The wave functions  $|\psi_p\rangle$  which are solutions of the equation

$$H_{\text{el}} |\psi_p\rangle = E_p |\psi_p\rangle$$

are characterized by free-ion-level quantum numbers  $aLSJ$ , an irreducible representation of the RE-ion site symmetry group  $G_s$ , and a row of this representation.

The lattice vibration Hamiltonian  $H_{\text{vib}}$  is invariant under the operations of the crystal space group  $G$ . The vibrational wave functions are characterized by irreducible representations of this group. The harmonic approximation is assumed here, and therefore, the Hamiltonian is a sum of harmonic-oscillator Hamiltonians for each normal coordinate:

$$H_{\text{vib}} = \sum_{k\gamma s} \left\{ -\frac{1}{2} \hbar^2 \nabla^2 Q_{k\gamma^s} + \frac{1}{2} \omega_{k\gamma}^2 Q_{k\gamma^s} Q_{k\gamma^{s*}} \right\}. \quad (3)$$

The normal coordinates  $Q_{k\gamma^s}$  are characterized by a wave vector  $\mathbf{k}$ , a small representation  $\gamma$ , and a row  $s$  of this representation. The Schrödinger equation for the normal coordinate  $Q_{k\gamma^s}$  is

$$\begin{aligned} & \left( -\frac{1}{2} \hbar^2 \nabla^2 Q_{k\gamma^s} + \frac{1}{2} \omega_{k\gamma}^2 Q_{k\gamma^s} Q_{k\gamma^{s*}} \right) | Q_{k\gamma^s} n_{k\gamma} \rangle \\ & = \left( n_{k\gamma} + \frac{1}{2} \right) \hbar \omega_{k\gamma} | Q_{k\gamma^s} n_{k\gamma} \rangle. \end{aligned} \quad (4)$$

The wave function for the whole system of phonons is

$$\prod_{k\gamma s} | Q_{k\gamma^s} n_{k\gamma} \rangle$$

TABLE I. Vibrational frequencies, polarization, intensity, and Zeeman effect of vibronic transitions of Nd<sup>3+</sup> in NdCl<sub>3</sub>.

Phonon frequency <sup>a</sup> (cm <sup>-1</sup> )	Polarization and intensity <sup>b</sup>	s <sup>c</sup>	Polarization and intensity <sup>b</sup>	s <sup>c</sup>	Phonon frequency <sup>a</sup> (cm <sup>-1</sup> )	Polarization and intensity <sup>b</sup>	s <sup>c</sup>	Polarization and intensity <sup>b</sup>	s <sup>c</sup>
a. <sup>4</sup> I <sub>9/2</sub> (μ = ± $\frac{5}{2}$ , Γ <sub>10</sub> ) → <sup>2</sup> P <sub>1/2</sub> (μ = ± $\frac{1}{2}$ , Γ <sub>7,8</sub> )					b. <sup>4</sup> I <sub>9/2</sub> (μ = ± $\frac{5}{2}$ , Γ <sub>9,10</sub> ) → <sup>2</sup> D <sub>5/2</sub> (μ = ± $\frac{1}{2}$ , ± $\frac{3}{2}$ , ± $\frac{5}{2}$ ; Γ <sub>7,8</sub> , Γ <sub>11,12</sub> , Γ <sub>9,10</sub> )				
Zero phonon	σ	2.6	π	1.8	$\tilde{\nu}$ cm <sup>-1</sup>	μ = ± $\frac{1}{2}$	μ = ± $\frac{3}{2}$	μ = ± $\frac{5}{2}$	
14.2	π(m)		σ(m)	1.3	52.4	π(s); σ(m)			
73* d	σ(w)		π(s)	1.9	72.0		σ(m)		
77.6	σ(m)	2.1	π(w)		77.7	σ(m)	σ(s); π(w)	σ(s); π(m)	
83* d	σ(m)		π(w)		84*	σ(w)			
92.2	π(ss)	1.6	σ(w)	1.4	92.6	π(s); σ(w)			
98.4	σ(w)		π(s)	1.3	98.9	π(w)	σ(s); π(w)		
104.4	σ(w)	1.9	π(m)	1.7	104.4	σ(s); π(w)	σ(s); π(s)	σ(m); π(w)	
110*			π(m)	1.7	119.7	σ(m); π(w)			
119.9			σ(w)	1.8	124.1		π(s); σ(w)		
123.8 <sup>e</sup>	π(s)		σ(s)		130.0	σ(m); π(w)	σ(m); π(m)		
129* <sup>e</sup>	π(m)		σ(m)		137.0		σ(s)		
134*	σ(s)	2.9	π(m)		142.5		π(m)		
138.8	σ(ss)	2.3	π(ss)	2.0	157.0	σ(w); π(m)		σ(m)	
143* f	σ(m)		π(m)		160.6	σ(s); π(s)			
156.0	π(ss)	2.2	σ(m)	1.6	161*		π(m); σ(m)		
160.8	π(ss)	1.9	σ(ss)	1.1	164.2		σ(s)		
166.5	π(ss)	2.0	σ(s)	1.6	167.0	σ(m); π(m)	σ(m); π(m)		
169.8			σ(w)	1.8	182.4		π(m); σ(m)		
172.6	σ(w)	1.7	π(m)	1.5	206.6	σ(m)			
181.5	σ(m)	1.9	π(w)		215*		σ(m); π(w)		
187.1	σ(w)	2.7	π(m)	2.0	239.3	π(m); σ(w)			
192.0	σ(m)	2.0	π(m)	1.6	254*		σ(w)		
196*			σ(m)	1.8	257*	π(s); σ(m)			
201.1	π(m)	1.7	σ(m)	1.6	c. <sup>4</sup> I <sub>9/2</sub> (μ = ± $\frac{5}{2}$ ; Γ <sub>9,10</sub> ) → <sup>2</sup> P <sub>3/2</sub> (μ = ± $\frac{1}{2}$ , ± $\frac{3}{2}$ ; Γ <sub>7,8</sub> , Γ <sub>11,12</sub> )				
205.6	σ(m)	1.9	π(m)	1.7	$\tilde{\nu}$ cm <sup>-1</sup>	μ = ± $\frac{1}{2}$	μ = ± $\frac{3}{2}$		
210*	σ(w)		π(w)	1.5	98.2		σ(w); π(w)		
217* g	σ(w)		π(w)		104.9		σ(w); π(w)		
223* g	σ(w)	1.3	π(w)	1.7	154.1		π(w)		
227*			σ(w)	1.0	156.1	σ(w); π(w)			
229.9			π(w)	0.8	160.4	σ(w); π(w)	π(m)		
234*	π(m)	1.8	σ(m)	1.7	165.2	σ(s); π(s)			
239.3	π(w)				166.3		π(m); σ(s)		
254*	π(ss)		σ(m)		223.5	σ(m)			
257* h	π(ss)		σ(m)		234.0		σ(s)		
264*	π(w)		σ(w)		259.3		π(w)		
					266.0	π(w)	π(w)		
					271.6		π(w)		

<sup>a</sup> Whenever an asterisk is given with the phonon frequency it indicates that the frequency measurement has a precision greater than ±1 cm<sup>-1</sup>. All other frequencies have a precision between ±0.1 and ±0.5 cm<sup>-1</sup>.

<sup>b</sup> The degrees of intensities are indicated by: ss=very strong, s=strong, m=medium, w=weak.

<sup>c</sup> s gives the slope of the magnetic energy versus magnetic field in Lorentz units.

<sup>d</sup> Broad band in σ (~10 cm<sup>-1</sup>).

<sup>e</sup> Anomalous Zeeman effect.

<sup>f</sup> Strong band in the region 134–143 cm<sup>-1</sup>.

<sup>g</sup> Broad band (~5 cm<sup>-1</sup>).

<sup>h</sup> Strong band in the region 250–260 cm<sup>-1</sup>.

and the corresponding energy is

$$\sum_{k\gamma s} (n_{k\gamma} + \frac{1}{2}) \hbar \omega_{k\gamma}.$$

The displacements  $x_i(n; \alpha)$ ,  $i=1, 2, 3$ , of the  $\alpha$ th ion in the  $n$ th unit cell are related to the normal coordinates by the transformation

$$x_i(n; \alpha) = \sum_{k\gamma s} (Nm_\alpha)^{-1/2} \eta_{i\gamma s}(\mathbf{k}; \alpha) \exp(i\mathbf{k} \cdot \mathbf{R}_n) Q_{k\gamma s}. \quad (5)$$

If  $V$  is the total interaction hamiltonian between the RE ion and the rest of the ions in the crystal, then it can be expanded in terms of the displacements  $x_i(n; \alpha)$ :

$$V = V_0 + \sum_{n\alpha i} x_i(n; \alpha) \nabla_i(n; \alpha) V + \dots \quad (6)$$

The first term is the electrostatic part which is incorporated with  $H_{el}$  [Eq. (2)]. In the second term, the derivatives are evaluated at the equilibrium posi-

TABLE II. Vibrational frequencies, polarization, intensity, and Zeeman effect of vibronic transitions of  $\text{Pr}^{3+}$  in  $\text{NdCl}_3$ .<sup>a</sup>

${}^3H_4(\mu = \pm 2, \Gamma_{2,s}) \rightarrow {}^3P_0(\mu = 0, \Gamma_1)$				
$\tilde{\nu}(\text{cm}^{-1})$	Polarization	$\tilde{\nu}(\text{cm}^{-1})$	Polarization	
77.7	$\sigma(\text{ss})$	163*	$\sigma(\text{s})$	
81.5	$\sigma(\text{s})$	166.9	$\pi(\text{m})$	
92.0	$\sigma(\text{w})$	172.1	$\sigma(\text{w})$	
98.5	$\sigma(\text{w})$	181.0	$\sigma(\text{w})$	
104.6	$\sigma(\text{m})$	188.5	$\sigma(\text{s})$	
110*	$\sigma(\text{w})$	194.1	$\sigma(\text{m})$	
123.9	$\sigma(\text{s})$	197*	$\sigma(\text{w})$	
129.4	$\sigma(\text{m}); \pi(\text{w})$	202.3	$\sigma(\text{m})$	
141*	$\sigma(\text{m})$	209.7	$\sigma(\text{s})$	
154.6	$\sigma(\text{m})$	217*	$\sigma(\text{m})$	
156.3	$\pi(\text{m})$	221*	$\sigma(\text{w})$	
159*	$\sigma(\text{w})$	238*	$\sigma(\text{m})$	
160.4	$\pi(\text{m})$	250*	$\sigma(\text{s})$	
		259*	$\sigma(\text{m})$	
${}^3H_4(\mu = \pm 2, \Gamma_{2,s}) \rightarrow {}^3P_2(\mu = 0, \Gamma_1)$				
$\tilde{\nu}(\text{cm}^{-1})$	Polarization	$\tilde{\nu}(\text{cm}^{-1})$	Polarization	
65*	$\sigma(\text{w})$	104.6	$\sigma(\text{s}); \pi(\text{w})$	
77.6	$\sigma(\text{s})$	154.7	$\sigma(\text{w})$	
82.1	$\sigma(\text{m})$	155.7	$\pi(\text{m})$	
91.9	$\sigma(\text{w})$	163.2	$\sigma(\text{w})$	
94.7	$\sigma(\text{w})$	166*	$\pi(\text{m})$	
98.2	$\sigma(\text{m})$	173*	$\sigma(\text{w}); \pi(\text{w})$	
		223*	$\sigma(\text{w})$	
${}^3H_4(\mu = \pm 2, \Gamma_{2,s}) \rightarrow {}^3P_2(\mu = \pm 1, \Gamma_{1,s})$				
$\tilde{\nu}(\text{cm}^{-1})$	$\mu = -1$	$s$	$\mu = +1$	$s$
Zero phonon	$\pi$	-1.79	$\pi$	+1.75
36.8	$\pi(\text{w})$	-1.4	$\pi(\text{w})$	0.9
37.6	$\sigma(\text{w})$		$\sigma(\text{m})$	1.3
70.9	$\pi(\text{w}); \sigma(\text{w})$	-1.8	$\pi(\text{w})$	1.2
77.9	$\pi(\text{s}); \sigma(\text{w})$	-1.2	$\pi(\text{s}); \sigma(\text{w})$	1.2
92.2	$\pi(\text{w})$	-1.9	$\pi(\text{w})$	1.7
97.4	$\pi(\text{m})$	-1.1	$\pi(\text{m})$	1.7
98.0	$\sigma(\text{w})$		$\sigma(\text{w})$	1.8
104.5	$\pi(\text{s})$	-1.3	$\pi(\text{w})$	1.0
111*	$\pi(\text{m})$	-1.1	$\pi(\text{m})$	1.0
119.5	$\pi(\text{w})$	-0.8	$\pi(\text{m}); \sigma(\text{w})$	2.1
123*	$\pi(\text{w})$		$\pi(\text{s})$	2.9
129*			$\pi(\text{m})$	2.0
130.1			$\sigma(\text{m})$	1.3
139.3	$\pi(\text{w})$		$\pi(\text{s})$	1.5
156.0	$\sigma(\text{w})$		$\sigma(\text{w})$	1.9
158.7	$\pi(\text{m})$	-2.3	$\pi(\text{m})$	1.9
160.9	$\sigma(\text{w})$		$\sigma(\text{s})$	1.7
166.3	$\sigma(\text{m})$		$\sigma(\text{m})$	2.3
172.4	$\pi(\text{m})$		$\pi(\text{m})$	1.0
187.3	$\sigma(\text{s}); \pi(\text{w})$	-1.7	$\sigma(\text{s}); \pi(\text{w})$	2.0
200.3	$\sigma(\text{m}); \pi(\text{w})$	-1.3	$\pi(\text{w})$	
205.3	$\pi(\text{s}); \sigma(\text{w})$	-1.5	$\pi(\text{s}); \sigma(\text{w})$	2.2
219.2	$\pi(\text{s})$	-1.5	$\pi(\text{s})$	2.1
254*	$\pi(\text{m})$		$\pi(\text{m})$	
${}^3H_4(\mu = \pm 2, \Gamma_{2,s}) \rightarrow {}^3P_2(\mu = \pm 2, \Gamma_{2,s})$				
$\tilde{\nu}(\text{cm}^{-1})$	$\mu = -2$	$s$	$\mu = +2$	$s$
Zero phonon	$\sigma$	-3.04	$\sigma$	3.08
72.8	$\sigma(\text{m})$	-2.5	$\sigma(\text{m})$	2.0
77.8	$\sigma(\text{s})$	-2.5	$\sigma(\text{s})$	
83.8			$\sigma(\text{s})$	2.6
87*			$\sigma(\text{m})$	2.4
92*	$\sigma(\text{m})$		$\sigma(\text{m})$	2.1
104*	$\sigma(\text{m}); \pi(\text{w})$	-2.3	$\sigma(\text{m}); \pi(\text{w})$	4.0
119.4	$\sigma(\text{w})$	-2.1	$\sigma(\text{s})$	2.3
124*	$\sigma(\text{w})$		$\sigma(\text{m})$	2.6
156*	$\pi(\text{m})$		$\pi(\text{m})$	
161.3	$\pi(\text{s})$	-4.0	$\pi(\text{s})$	2.3
167.4	$\pi(\text{s})$		$\pi(\text{s})$	2.6
172*	$\sigma(\text{w})$		$\sigma(\text{w})$	
198*	$\sigma(\text{w})$		$\sigma(\text{w})$	
205*	$\pi(\text{w})$		$\pi(\text{w})$	
240*	$\pi(\text{w})$		$\pi(\text{w})$	2.4
254*	$\sigma(\text{m})$		$\sigma(\text{m})$	

<sup>a</sup> For explanation of symbols see Table I.

tions of all ions, with the RE ion considered located at the origin.

By virtue of Eq. (4), the interaction Hamiltonian between RE ion and the lattice vibrations has the form

$$\begin{aligned}
 V_{\text{ev}} &= \sum_{n\alpha i} x_i(n; \alpha) \nabla_i(n; \nabla) V \\
 &= \sum_{k\gamma s} \left[ \sum_{n\alpha i} (Nm_\alpha)^{-1/2} \eta_{i\gamma s}(\mathbf{k}; \alpha) \right. \\
 &\quad \left. \times \exp(i\mathbf{k} \cdot \mathbf{R}_n) \nabla_i(n; \alpha) V \right] \cdot Q_{k\gamma}^s \\
 &= \sum_{k\gamma s} f_{k\gamma}^s Q_{k\gamma}^s. \tag{7a}
 \end{aligned}$$

The operators  $f_{k\gamma}^s$ , defined by the last equation, operate on the RE-ion electronic states only, while  $Q_{k\gamma}^s$  operate on the phonon states only. Such a separation in  $V_{\text{ev}}$  is valid under the aforementioned assumptions, namely:  $V_{\text{ev}} \ll V_0$  and  $V_{\text{ev}} \ll H_{\text{vib}}$ . Invoking the assumption of a single RE ion interacting with the lattice vibrations implies that  $V_{\text{ev}}$  is not invariant under the space-group operations, but rather under the operations of the ion-site symmetry group  $G_s$ . For the case of an impurity ion (substituting another RE ion which is a natural constituent of the crystal) this assumption holds automatically. However, it is found experimentally that it holds also for  $\text{Nd}^{3+}$  in  $\text{NdCl}_3$ . A comparison between the vibronic spectrum of  $\text{Nd}^{3+}$  in  $\text{LaCl}_3$  and  $\text{NdCl}_3$  shows that the spectra are similar except for small shifts of the phonon energies. This means that the electronic excitation is sufficiently localized to single out the RE ion undergoing a vibronic transition. Consequently, the phonon wave functions which transform according to the irreducible representations of  $G$  are combined into linear combinations which form a basis for the irreducible representations of  $G_s$ , ( $G - G_s$ ). Applying this procedure to the lattice normal coordinates  $Q_{k\gamma}^s$ , the following expression is obtained for  $V_{\text{ev}}$ :

$$V_{\text{ev}} = \sum_{\mathbf{k}\Gamma^s} f_{\mathbf{k}\Gamma^s} Q_{\mathbf{k}\Gamma^s}^s. \tag{7b}$$

While the sum over  $\mathbf{k}$  in Eq. (7a) implies a sum over all vectors in the star of  $\mathbf{k}$ , the sum symbol  $\mathbf{k}$  in Eq. (7b) stands for a single vector representing the star of  $\mathbf{k}$ . The sum extends over all distinct stars in the B.Z., over all irreducible representations  $\Gamma$  of  $G_s$  which appear in the reduction  $G \rightarrow G_s$  and over all the rows of these representations. The operator  $f_{\mathbf{k}\Gamma^s}$  belongs to the same  $\Gamma$  as  $Q_{\mathbf{k}\Gamma^s}$  for a real representation and to  $\Gamma^*$  for a complex one.

In obtaining the wave functions for the coupled system we assume the limit of  $T = 0^\circ\text{K}$ , so that the initial vibrational state is the ground state:

$$\prod_{\mathbf{k}\Gamma^s} |Q_{\mathbf{k}\Gamma^s}^s 0\rangle.$$

The vibronic state corresponding to excitation of no

phonons is given by first-order perturbation theory:

$$|\chi_a^0\rangle = |\psi_a\rangle \sum_{\mathbf{k}\Gamma_s} |Q_{\mathbf{k}\Gamma^s 0}\rangle + \sum_p \left\{ |\psi_p\rangle \sum_{\mathbf{k}\Gamma_s} \left[ \left( \frac{\hbar}{2\omega_{\mathbf{k}\Gamma}} \right)^{1/2} \frac{\langle \psi_p | f_{\mathbf{k}\Gamma^s} | \psi_a \rangle}{E_a - (E_p + \hbar\omega_{\mathbf{k}\Gamma})} \prod_{\mathbf{k}'\Gamma'^{s'}} |Q_{\mathbf{k}'\Gamma'^{s'} 0}\rangle |Q_{\mathbf{k}\Gamma^s 1}\rangle \right] \right\}. \quad (8)$$

The vibronic state corresponding to a single excited phonon of the mode ( $\mathbf{k}\Gamma_s$ ) is given by

$$|\chi_a^1\rangle = |\psi_a\rangle \prod_{\mathbf{k}'\Gamma'^{s'}} |Q_{\mathbf{k}'\Gamma'^{s'} 0}\rangle |Q_{\mathbf{k}\Gamma^s 1}\rangle + \sum_p \left\{ |\psi_p\rangle \sum_{\mathbf{k}'\Gamma'^{s''}} \left[ \left( \frac{\hbar}{2\omega_{\mathbf{k}'\Gamma''}} \right)^{1/2} \frac{\langle \psi_p | f_{\mathbf{k}'\Gamma''^{s''}} | \psi_a \rangle}{(E_a + \hbar\omega_{\mathbf{k}\Gamma}) - (E_p + \hbar\omega_{\mathbf{k}'\Gamma''})} \right. \right. \\ \left. \left. + \prod_{\mathbf{k}'\Gamma'^{s'}} |Q_{\mathbf{k}'\Gamma'^{s'} 0}\rangle |Q_{\mathbf{k}'\Gamma''^{s''} 1}\rangle |Q_{\mathbf{k}\Gamma^s 1}\rangle \right] \right\} + \sum_p \left[ |\psi_p\rangle \left( \frac{\hbar}{2\omega_{\mathbf{k}\Gamma}} \right)^{1/2} \frac{\langle \psi_p | f_{\mathbf{k}\Gamma^s} | \psi_a \rangle}{(E_a + \hbar\omega_{\mathbf{k}\Gamma}) - E_p} \prod_{\mathbf{k}\Gamma^s} |Q_{\mathbf{k}\Gamma^s 0}\rangle \right]. \quad (9)$$

The energy correction to the energy  $E_a$  of the state  $|\chi_a^0\rangle$  which is due to  $V_{ev}$  is given by the expression

$$\Delta E^0 = \sum_p \sum_{\mathbf{k}\Gamma_s} \frac{\hbar}{2\omega_{\mathbf{k}\Gamma}} \frac{|\langle \psi_p | f_{\mathbf{k}\Gamma^s} | \psi_a \rangle|^2}{E_a - (E_p + \hbar\omega_{\mathbf{k}\Gamma})}.$$

The state  $|\chi_a^1\rangle$  has a zeroth-order energy  $E_a + \hbar\omega_{\mathbf{k}\Gamma}$  and the energy correction due to  $V_{ev}$  is  $\Delta E^1$ . The difference between these corrections is given by

$$\delta = \Delta E^1 - \Delta E^0 = \sum_p \frac{\hbar}{2\omega_{\mathbf{k}\Gamma}} \frac{|\langle \psi_p | f_{\mathbf{k}\Gamma^s} | \psi_a \rangle|^2}{(E_a + \hbar\omega_{\mathbf{k}\Gamma}) - E_p}. \quad (10)$$

This quantity can be estimated from the observed small variations of the vibronic energies corresponding to a given phonon with different electronic levels.

### b. Vibronic Transition Probabilities

At the low-temperature limit vibronic transitions involve creation of phonons only. The electric dipole matrix element  $\langle \chi_a^0 | P^{[1]} | \chi_b^1 \rangle$  corresponds to a transition of the RE ion from state  $a$  to state  $b$  plus a creation of one phonon of the mode ( $\mathbf{k}\Gamma_s$ ). Using Eqs. (8) and (9), the explicit form of this matrix element is obtained in first approximation:

$$\langle \chi_a^0 | P^{[1]} | \chi_b^1 \rangle = \sum_p \left( \frac{\hbar}{2\omega_{\mathbf{k}\Gamma}} \right)^{1/2} \left[ \frac{\langle \psi_a | f_{\mathbf{k}\Gamma^s} | \psi_p \rangle \langle \psi_p | P^{[1]} | \psi_b \rangle}{E_a - (E_p + \hbar\omega_{\mathbf{k}\Gamma})} + \frac{\langle \psi_a | P^{[1]} | \psi_p \rangle \langle \psi_p | f_{\mathbf{k}\Gamma^s} | \psi_b \rangle}{(E_b + \hbar\omega_{\mathbf{k}\Gamma}) - E_p} \right]. \quad (11)$$

The initial state  $|\chi_a^0\rangle$  involves the phonon ground state which belongs to the identity representation of both  $G$  and  $G_s$ . Therefore,  $|\chi_a^0\rangle$  belongs to the same  $\Gamma_a$  as  $|\psi_a\rangle$ . The state  $|\chi_b^1\rangle$  involves the electronic state  $|\psi_b\rangle$  which belongs to  $\Gamma_b$  and a phonon state which belongs to a representation  $\Gamma$  of  $G_s$ . Therefore,  $|\chi_b^1\rangle$  belongs to  $\Gamma \times \Gamma_b$ .

If the components of  $P^{[1]}$  transform like  $\Gamma_i$  ( $i = x, y, z$ ) then the selection rules for vibronic transitions are

$$\langle \chi_a^0 | P_i^{[1]} | \chi_b^1 \rangle = 0$$

$$\text{if } \Gamma_a \times \Gamma \times \Gamma_b \text{ does not contain } \Gamma_i. \quad (12)$$

The transition probability per unit time is given by

$$W = (2\pi/\hbar) |\langle \chi_a^0 | P^{[1]} | \chi_b^1 \rangle|^2 \rho(E). \quad (13)$$

The density of final states  $\rho(E)$  is the product of the phonon density of states  $g(\omega)$  and the density of final electronic states  $\rho(E - \hbar\omega)$ . Since the energy spread of the electronic states is much smaller than that of the phonon states, for the case studied here, one can take  $\rho(E - \hbar\omega) = \delta(E - \hbar\omega - E_b)$ . Then, the vibronic spectrum reflects the structure of  $g(\omega)$ . Vibronic transitions are observed at those phonon energies  $\hbar\omega$  where  $g(\omega)$

has peaks. The relative strength of the transitions, however, does not necessarily accurately indicate the actual relative strength of the peaks of  $g(\omega)$  since the coupling coefficients  $\langle \psi_a | f_{\mathbf{k}\Gamma^s} | \psi_p \rangle$  which appears in the expression for  $W$  may differ. If a vibronic line (or band) shows a certain degree of polarization then the corresponding peak of  $g(\omega)$  is attributed to phonons which have  $\hbar$  along directions of high symmetry in the B.Z.

### c. The Interaction with Acoustical Phonons

The expression for  $\langle \chi_a^0 | P^{[1]} | \chi_b^1 \rangle$  in Eq. (11) consists of contributions from all intermediate electronic states  $p$ . If the dominant term is that for which  $p = a$ , then one obtains

$$\langle \chi_a^0 | P^{[1]} | \chi_b^1 \rangle \approx \langle \psi_a | P^{[1]} | \psi_b \rangle \\ \times \left( \frac{\hbar}{2\omega_{\mathbf{k}\Gamma}} \right)^{1/2} \left( \frac{\langle \psi_a | f_{\mathbf{k}\Gamma^s} | \psi_a \rangle}{-\hbar\omega_{\mathbf{k}\Gamma}} + \frac{\langle \psi_b | f_{\mathbf{k}\Gamma^s} | \psi_b \rangle}{\hbar\omega_{\mathbf{k}\Gamma}} \right). \quad (14)$$

In this case the vibronic transition probability is proportional to that of the parent electronic transition and the vibronic band will have, therefore, the same polarization as its parent. Such a behavior is observed

TABLE III. Space-group reduction coefficients:  $C_{6h}^2 \rightarrow C_{3h}$ .

	$\Gamma_1$	$\Gamma_2$	$\Gamma_3$	$\Gamma_4$	$\Gamma_5$	$\Gamma_6$		$\Gamma_1$	$\Gamma_2$	$\Gamma_3$	$\Gamma_4$	$\Gamma_5$	$\Gamma_6$
$L_1$	1	1	1	1	1	1	$\Delta_3$			1			1
$T_1$	2	2	2				$\Delta_4$		1			1	
$T_2$				2	2	2	$\Delta_5$		1			1	
$U_1$	1	1	1	1	1	1	$\Delta_6$			1			1
$U_2$	1	1	1	1	1	1	$\Gamma_1^+$	1					
$P_1$	2			2			$\Gamma_2^+$		1				
$P_2$			2			2	$\Gamma_3^+$			1			
$P_3$		2			2		$\Gamma_4^+$				1		
$M_1$	1	1	1				$\Gamma_5^+$					1	
$M_2$				1	1	1	$\Gamma_6^+$						1
$M_3$	1	1	1				$\Gamma_1^-$				1		
$M_4$				1	1	1	$\Gamma_2^-$					1	
$K_1$	2						$\Gamma_3^-$						1
$K_2$		2					$\Gamma_4^-$	1					
$K_3$			2				$\Gamma_5^-$		1				
$K_4$				2			$\Gamma_6^-$			1			
$K_5$					2		$A_1$	1			1		
$K_6$						2	$A_2$			1			1
$\Delta_1$	1			1			$A_3$	2	1		2	1	
$\Delta_2$	1			1			$k^a$	2	2	2	2	2	2

<sup>a</sup> General point  $k$ .

for vibronic bands due to acoustical phonons which accompany transitions to Stark manifolds with only one isolated component. It should be noted that many vibronic transitions due to optical phonons appear with a polarization opposite to that of their parent transition, indicating the importance of all the terms in Eq. (11). It was also observed that the intensity of the acoustical phonon vibronic band was linearly dependent on the phonon energy. In order to account for such a behavior one notes that the "polarization vectors"  $m_a^{-1/2}\eta_{i\Gamma_s}(\mathbf{k}; \alpha)$  are approximately equal for all ions in the vicinity of the RE ion for acoustical modes and  $\mathbf{k} \approx 0$ . Also, the crystal field

$$V = \sum_{n,\alpha} V(n; \alpha)$$

is a sum of the contributions of all the ions in the crystal except the RE ion considered. The gradient of  $V$  with respect to the RE ion (located at the origin) can be written as  $\nabla_i(0; 0)V(n; \alpha) = -\nabla_i(n; \alpha)V(n; \alpha)$ . Using all these for  $f_{k\Gamma^s}$  of Eq. (7a) one obtains the approximation

$$f_{k\Gamma^s} \approx \sum_{n\alpha i} (Nm_\alpha)^{-1/2} \eta_{i\Gamma_s}(\mathbf{k}; \alpha) (i\mathbf{k} \cdot \mathbf{R}_n) \nabla_i(n; \alpha) V \\ \equiv \sum_i \frac{\omega_{k\Gamma}}{C_{\Gamma_i}(\mathbf{k})} f_{k\Gamma_i^s}. \quad (15)$$

$$\epsilon = \sum_p \frac{\hbar}{2\omega_{k\Gamma}} \frac{|\langle \psi_p | f_{k\Gamma^s} | \psi_a \rangle|^2}{(E_a + \hbar\omega_{k\Gamma}) - E_p} + \sum_{p \neq a} \sum_{p'} \frac{\hbar}{2\omega_{k\Gamma}} \frac{\langle \psi_a | f_{k\Gamma^s} | \psi_{p'} \rangle \langle \psi_{p'} | f_{k\Gamma^s} | \psi_p \rangle \langle \psi_p | H_m | \psi_a \rangle}{[(E_a + \hbar\omega_{k\Gamma}) - E_{p'}](E_a - E_p)} \\ + \sum_p \sum_{p'} \frac{\hbar}{2\omega_{k\Gamma}} \frac{\langle \psi_a | f_{k\Gamma^s} | \psi_{p'} \rangle \langle \psi_{p'} | H_m | \psi_p \rangle \langle \psi_p | f_{k\Gamma^s} | \psi_a \rangle}{[(E_a + \hbar\omega_{k\Gamma}) - E_{p'}][(E_a + \hbar\omega_{k\Gamma}) - E_p]}. \quad (17)$$

The contribution of the RE ion is excluded from the sum.  $C_{\Gamma_i}(\mathbf{k})$  is the sound velocity for the branch  $\Gamma$ . Using Eq. (14) and assuming an average velocity  $C_i$ , and average value  $f_i$  for the two acoustical branches for all  $\mathbf{k} \sim 0$ , and  $g(\omega) \sim \omega^2$ , one obtains the transition rate from electronic state  $a$  to state  $b$  involving the creation of acoustical phonons with energies between  $\hbar\omega$  and  $\hbar(\omega + d\omega)$ :

$$W = \frac{\omega}{2\pi\hbar} |\langle \psi_a | P^{[1]} | \psi_b \rangle|^2 \\ \times \sum_i \frac{|\langle \psi_a | f_i | \psi_a \rangle - \langle \psi_b | f_i | \psi_b \rangle|^2}{C_i^5}. \quad (16)$$

Such a behavior was found by Hobden<sup>5</sup> for  $\text{Eu}^{2+}$  in  $\text{CaF}_2$ . Other types of dependence were observed<sup>12</sup> for  $\text{Cr}^{3+}$  in  $\text{Al}_2\text{O}_3$  and  $\text{V}^{2+}$  in  $\text{MgO}$ .

#### d. The Zeeman Effect of Vibronic States

The application of an external magnetic field  $\mathbf{H}$  introduces the term  $H_m = -\mu_B(\mathbf{J} + \mathbf{S}) \cdot \mathbf{H}$  into the Hamiltonian of Eq. (1). A given zero-phonon Kramers doublet

$$|\psi_a\rangle \prod_{k\Gamma_s} |Q_{k\Gamma^s} 0\rangle \quad \text{and} \quad |\tilde{\psi}_a\rangle \prod_{k\Gamma_s} |Q_{k\Gamma^s} 0\rangle$$

will split under the applied field. If  $\langle \psi_a | H_m | \tilde{\psi}_a \rangle = 0$ , the states will have the energies

$$E_a + \langle \psi_a | H_m | \psi_a \rangle \quad \text{and} \quad E_a + \langle \tilde{\psi}_a | H_m | \tilde{\psi}_a \rangle,$$

respectively. Similarly, the single excited phonon vibronic states

$$|\psi_a\rangle \prod_{k'\Gamma^{s'}} |Q_{k'\Gamma^{s'}} 0\rangle |Q_{k\Gamma^s} 1\rangle$$

and

$$|\tilde{\psi}_a\rangle \prod_{k'\Gamma^{s'}} |Q_{k'\Gamma^{s'}} 0\rangle |Q_{k\Gamma^s} 1\rangle$$

will have the zeroth-order energies  $E_a + \hbar\omega_{k\Gamma} + \langle \psi_a | H_m | \psi_a \rangle$  and  $E_a + \hbar\omega_{k\Gamma} + \langle \tilde{\psi}_a | H_m | \tilde{\psi}_a \rangle$ , respectively. Therefore, in the zeroth approximation, the vibronic states will have the same splitting factor as their parent electronic states. Using the expressions for  $|\chi_a^0\rangle$  and  $|\chi_a^1\rangle$ , Eqs. (8) and (9), the energy corrections due to both  $H_m$  and  $V_{ev}$  can be obtained. The quantity of interest is the deviation of the energy of the single excited phonon vibronic state from the energy of the corresponding zero phonon state. This quantity has the form

<sup>12</sup> S. E. Stokowski, S. A. Johnson, and P. L. Scott, Phys. Rev. **147**, 544 (1966); L. A. Vredevoe, *ibid.* **147**, 541 (1966).

TABLE IV. Compatibility relations for  $C_{6h}^2$ .

$\Gamma_1^+$	$\Gamma_2^+$	$\Gamma_3^+$	$\Gamma_4^+$	$\Gamma_5^+$	$\Gamma_6^+$	$\Gamma_1^-$	$\Gamma_2^-$	$\Gamma_3^-$	$\Gamma_4^-$	$\Gamma_5^-$	$\Gamma_6^-$
$\Delta_1$	$\Delta_4$	$\Delta_5$	$\Delta_2$	$\Delta_5$	$\Delta_6$	$\Delta_1$	$\Delta_4$	$\Delta_3$	$\Delta_2$	$\Delta_5$	$\Delta_6$
$T_1$	$T_1$	$T_1$	$T_2$	$T_2$	$T_2$	$T_2$	$T_2$	$T_2$	$T_1$	$T_1$	$T_1$
$\Sigma_1$	$\Sigma_1$	$\Sigma_1$	$\Sigma_2$	$\Sigma_2$	$\Sigma_2$	$\Sigma_2$	$\Sigma_3$	$\Sigma_2$	$\Sigma_1$	$\Sigma_1$	$\Sigma_1$
$K_1$	$K_2$	$K_3$	$K_4$	$K_4$	$K_6$	$K_6$		$A_1$	$A_2$	$A_3$	
$T_1$	$T_1$	$T_1$	$T_2$	$T_2$	$T_2$	$T_2$		$\Delta_1, \Delta_2$	$\Delta_3, \Delta_6$	$\Delta_4, \Delta_5$	
$P_1$	$P_3$	$P_2$	$P_1$	$P_3$	$P_3$	$P_2$		$S_1, S_2$	$S_1, S_2$	$S_1, S_2$	
								$R_1, R_2$	$R_1, R_2$	$R_1, R_2$	
$M_1$	$M_2$	$M_3$	$M_4$			$H_1$	$H_2$	$H_3$	$H_4$	$H_5$	$H_6$
$T_1$	$T_2$	$T_1$	$T_2$			$S_1$	$S_1$	$S_1$	$S_2$	$S_2$	$S_2$
$U_1$	$U_2$	$U_2$	$U_1$			$P_1$	$P_3$	$P_2$	$P_1$	$P_3$	$P_2$
$T_1'$	$T_2'$	$T_1'$	$T_2'$								
$\Sigma_1$	$\Sigma_2$	$\Sigma_1$	$\Sigma_2$								

The first term represents a shift independent of the magnetic field [cf. Eq. (10)]. The last two terms are linear in the magnetic field and represent a deviation of the splitting factor of the state  $|\chi_a^1\rangle$  from that of  $|\chi_a^0\rangle$ .

#### IV. APPLICATION TO $NdCl_3$

$NdCl_3$  belongs to the space group  $C_{6h}^2(P6_3/m)$ . There are two formula units per unit cell and the RE ions are located at sites of  $C_{3h}$  point symmetry. Following Satten,<sup>7</sup> the reduction coefficients  $C_{6h}^2 \rightarrow C_{3h}$  are obtained for all points and directions of high symmetry in the B.Z. (see Fig. 4). The results are compiled in Table III.<sup>13</sup> It should be noted that the groups of the vector  $\mathbf{k}$  for the points  $K, K', H, H'$  are isomorphic, and so are those for the points  $T, T', \Sigma, S, S', R$ . Therefore, the space-group representations have the same reduction coefficients. Of special importance are the compatibility relations which are compiled in Table IV. Using these relations a phonon branch can be traced along a direction of high symmetry. If a vibronic line is due to

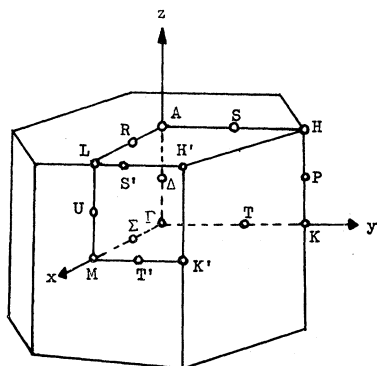


FIG. 4. Brillouin zone for the hexagonal Bravais lattice.

<sup>13</sup> The notation of the irreducible representations is that of G. E. Koster *et al.*, *Properties of the Thirty-Two Point Groups* (M.I.T. Press, Cambridge, Massachusetts, 1963).

a branch which is flat along a direction of high symmetry and it terminates at a point of a higher symmetry on the boundary of the B.Z., then a modification of the selection rules may happen, for different parts of the branch.

Using Eq. (12), the selection rules for vibronic transitions for the case of an ion with an odd number of electrons and a magnetic field parallel to the  $c$  axis are derived. The components of the electric dipole operator  $P^{[1]}$  transform as follows:

$$\begin{aligned}
 P_x^{[1]} \pm iP_y^{[1]} & \text{ like } \Gamma_2 \text{ and } \Gamma_3 \text{ of } C_{3h}, \\
 P_z^{[1]} & \text{ like } \Gamma_4 \text{ of } C_{3h}.
 \end{aligned}
 \quad (18)$$

Table V compiles the selection rules for vibronic transitions involving single phonons from the ground state of  $Nd^{3+}$  (which is  $\Gamma_{9,10}$  or  $\mu = \pm \frac{5}{2}$ ) to the various Stark components of the excited states. The selection rules for  $Pr^{3+}$  vibronics were derived by Satten<sup>7</sup> and were rederived by us for the case of an applied external magnetic field.<sup>14</sup>

From the table it is seen that the same vibronic selection rules are obtained for the following groups of points in the B.Z.:

- $\Gamma, K, K', H, H'$
- $T, T', \Sigma, S, S', R, M$
- $P$
- $\Delta, A$
- $L, U$  and any general point  $\mathbf{k}$ .

Also, it is apparent that no analysis of the vibronic spectrum can be done without having the Zeeman effect of the vibronic lines. In the case of zero magnetic field, transitions take place from the Kramers doublet  $\Gamma_{9,10}(\mu = \pm \frac{5}{2})$ , and most phonons will give rise to unpolarized vibronics (cf. Fig. 1). Upon applying an external magnetic field the transitions between the various Zeeman components of the vibronic states

<sup>14</sup> Elisha Cohen and H. W. Moos, following paper, *Phys. Rev.* **161**, 268 (1967).



TABLE V. Electric dipole selection rules for vibronic transitions originating at  $\Gamma_{9,10}$  ( $\mu = \pm \frac{5}{2}$ ) and terminating at the various electronic Stark components plus one quantum of vibration. (Magnetic field parallel to the  $c$  axis.)

	Transitions from $\Gamma_9$ ( $\mu = -\frac{5}{2}$ )						Transitions from $\Gamma_{10}$ ( $\mu = +\frac{5}{2}$ )					
	$\Gamma_7$ ( $\mu = +\frac{1}{2}$ )	$\Gamma_8$ ( $-\frac{1}{2}$ )	$\Gamma_9$ ( $-\frac{5}{2}$ )	$\Gamma_{10}$ ( $+\frac{5}{2}$ )	$\Gamma_{11}$ ( $-\frac{3}{2}$ )	$\Gamma_{12}$ ( $+\frac{3}{2}$ )	$\Gamma_7$ ( $\mu = +\frac{1}{2}$ )	$\Gamma_8$ ( $-\frac{1}{2}$ )	$\Gamma_9$ ( $-\frac{5}{2}$ )	$\Gamma_{10}$ ( $+\frac{5}{2}$ )	$\Gamma_{11}$ ( $-\frac{3}{2}$ )	$\Gamma_{12}$ ( $+\frac{3}{2}$ )
Zero phonon	$\pi$	$\sigma$	...	...	...	$\sigma$	$\sigma$	$\pi$	...	...	$\sigma$	...
$L_1$	$\sigma\pi$	$\sigma\pi$	$\sigma\pi$	$\sigma\pi$	$\sigma\pi$	$\sigma\pi$	$\sigma\pi$	$\sigma\pi$	$\sigma\pi$	$\sigma\pi$	$\sigma\pi$	$\sigma\pi$
$T_1$	$\pi$	$\sigma$	$\sigma$	$\pi$	$\pi$	$\sigma$	$\sigma$	$\pi$	$\pi$	$\sigma$	$\sigma$	$\pi$
$T_2$	$\sigma$	$\pi$	$\pi$	$\sigma$	$\sigma$	$\pi$	$\pi$	$\sigma$	$\sigma$	$\pi$	$\pi$	$\sigma$
$U_1$	$\sigma\pi$	$\sigma\pi$	$\sigma\pi$	$\sigma\pi$	$\sigma\pi$	$\sigma\pi$	$\sigma\pi$	$\sigma\pi$	$\sigma\pi$	$\sigma\pi$	$\sigma\pi$	$\sigma\pi$
$U_2$	$\sigma\pi$	$\sigma\pi$	$\sigma\pi$	$\sigma\pi$	$\sigma\pi$	$\sigma\pi$	$\sigma\pi$	$\sigma\pi$	$\sigma\pi$	$\sigma\pi$	$\sigma\pi$	$\sigma\pi$
$P_1$	$\pi$	$\sigma$	$\pi$	$\sigma$	$\sigma$	$\sigma$	$\sigma$	$\pi$	$\sigma$	$\pi$	$\sigma$	$\sigma$
$P_{2,3}$	$\sigma$	$\sigma\pi$	$\sigma$	$\sigma\pi$	$\sigma\pi$	$\sigma\pi$	$\sigma\pi$	$\sigma$	$\sigma\pi$	$\sigma$	$\sigma\pi$	$\sigma\pi$
$M_1, M_3$	$\pi$	$\sigma$	$\sigma$	$\pi$	$\pi$	$\sigma$	$\sigma$	$\pi$	$\pi$	$\sigma$	$\sigma$	$\pi$
$M_2, M_4$	$\sigma$	$\pi$	$\pi$	$\sigma$	$\sigma$	$\pi$	$\pi$	$\sigma$	$\sigma$	$\pi$	$\pi$	$\sigma$
$K_1$	$\pi$	$\sigma$	...	...	...	$\sigma$	$\sigma$	$\pi$	...	...	$\sigma$	...
$K_{2,3}$	...	$\sigma$	$\sigma$	$\pi$	$\pi$	$\sigma$	$\sigma$	...	$\sigma$	$\sigma$	$\sigma$	$\pi$
$K_4$	...	...	$\pi$	$\sigma$	$\sigma$	...	...	...	$\sigma$	$\pi$	...	$\sigma$
$K_{5,6}$	$\sigma$	$\pi$	...	$\sigma$	$\sigma$	$\pi$	$\pi$	$\sigma$	$\sigma$	...	$\pi$	$\sigma$
$\Delta_1$	$\pi$	$\sigma$	$\pi$	$\sigma$	$\sigma$	$\sigma$	$\sigma$	$\pi$	$\pi$	$\sigma$	$\sigma$	$\sigma$
$\Delta_2$	$\pi$	$\sigma$	$\pi$	$\sigma$	$\sigma$	$\sigma$	$\sigma$	$\pi$	$\sigma$	$\pi$	$\sigma$	$\sigma$
$\Delta_3$	$\sigma$	$\sigma$	$\sigma$	$\sigma$	$\pi$	$\pi$	$\pi$	$\sigma$	$\pi$	$\sigma$	$\sigma$	$\sigma$
$\Delta_4$	$\sigma$	$\pi$	$\sigma$	$\pi$	$\sigma$	$\sigma$	$\sigma$	$\sigma$	$\sigma$	$\pi$	$\pi$	$\pi$
$\Delta_5$	$\sigma$	$\pi$	$\sigma$	$\pi$	$\sigma$	$\sigma$	$\sigma$	$\sigma$	$\sigma$	$\sigma$	$\pi$	$\pi$
$\Delta_6$	$\sigma$	$\sigma$	$\sigma$	$\sigma$	$\pi$	$\pi$	$\pi$	$\sigma$	$\pi$	$\sigma$	$\sigma$	$\sigma$
$\Gamma_1^+$	$\pi$	$\sigma$	...	...	...	$\sigma$	$\sigma$	$\pi$	...	...	$\sigma$	...
$\Gamma_{2,3}^+$	...	$\sigma$	$\sigma$	$\pi$	$\pi$	$\sigma$	$\sigma$	...	$\pi$	$\sigma$	$\sigma$	$\pi$
$\Gamma_4^+$	...	...	$\pi$	$\sigma$	$\sigma$	...	...	...	$\sigma$	$\pi$	...	$\sigma$
$\Gamma_{5,6}^+$	$\sigma$	$\pi$	...	$\sigma$	$\sigma$	$\pi$	$\pi$	$\sigma$	$\sigma$	...	$\pi$	$\sigma$
$\Gamma_1^-$	...	...	$\pi$	$\sigma$	$\sigma$	...	...	...	$\sigma$	$\pi$	...	$\sigma$
$\Gamma_{2,3}^-$	$\sigma$	$\pi$	...	$\sigma$	$\sigma$	$\pi$	$\pi$	$\sigma$	$\sigma$	...	$\pi$	$\sigma$
$\Gamma_4^-$	$\pi$	$\sigma$	...	...	...	$\sigma$	$\sigma$	$\pi$	...	...	$\sigma$	...
$\Gamma_{5,6}^-$	...	$\sigma$	$\sigma$	$\pi$	$\pi$	$\sigma$	$\sigma$	...	$\pi$	$\sigma$	$\sigma$	$\pi$
$A_1$	$\pi$	$\sigma$	$\pi$	$\sigma$	$\sigma$	$\sigma$	$\sigma$	$\pi$	$\sigma$	$\pi$	$\sigma$	$\sigma$
$A_2$	$\sigma$	$\sigma$	$\sigma$	$\sigma$	$\pi$	$\pi$	$\pi$	$\sigma$	$\pi$	$\sigma$	$\sigma$	$\sigma$
$A_3$	$\sigma$	$\pi$	$\sigma$	$\pi$	$\sigma$	$\sigma$	$\sigma$	$\sigma$	$\sigma$	$\sigma$	$\pi$	$\pi$

become strongly polarized, thus providing more definite information on the phonon symmetries.

## V. DISCUSSION

### a. Acoustical Phonons

The broad vibronic absorption band in the phonon energies range of 0–80  $\text{cm}^{-1}$  which is associated with the transition  ${}^4I_{9/2}$  ( $\mu = \pm \frac{5}{2}$ )  $\rightarrow$   ${}^2P_{1/2}$  ( $\mu = \pm \frac{1}{2}$ ) of  $\text{Nd}^{3+}$  is attributed to the acoustical phonon branches around  $\mathbf{k}=0$  (Fig. 1). The absorption intensity is found to be linearly dependent on the phonon energy as predicted by theory [Eq. (16)]. Although the parent transition is unpolarized (at zero magnetic field), some polarization effects are observed in the vibronic band. The slope of the intensity versus phonon energy is constant up to 80  $\text{cm}^{-1}$  in the  $\sigma$  polarization. The slope in the  $\pi$  polarization changes at 40  $\text{cm}^{-1}$ : Up to 40  $\text{cm}^{-1}$  it is larger than that of the  $\sigma$  vibronic band, but from 40–80  $\text{cm}^{-1}$  it is close to that of the  $\sigma$  band. No apparent reason is seen for this behavior. A broad absorption band due to acoustical phonons is observed associated with the transition  ${}^3H_4$  ( $\mu = \pm 2$ )  $\rightarrow$   ${}^3P_0$  ( $\mu = 0$ ) of  $\text{Pr}^{3+}$ . It is strictly  $\sigma$  polarized and shows a linear dependence of the intensity on the phonon energy up to 75  $\text{cm}^{-1}$  where a strong peak is observed. The fact that this band follows the polarization of the parent electronic

transition ( $\sigma$ ) is, again, in agreement with Eq. (16). The intensity of the vibronic band due to acoustical phonon branches drops off around 80  $\text{cm}^{-1}$ . This value is close to the Debye temperature observed by Varsanyi<sup>15</sup> for  $\text{LaCl}_3$  ( $\theta = 149^\circ\text{K}$  which is equivalent to 105  $\text{cm}^{-1}$ ).

### b. Optical Phonons

From the observed polarization of a vibronic transition, using the selection rules compiled in Table V, a phonon branch is assigned to the vibration involved in the transition. In so doing it is assumed that all vibronics are due to single phonons. The vibronic lines have similar peak intensities and widths and the spectra cut off at 270  $\text{cm}^{-1}$  without a gradual weakening of the lines. The strongest vibronics appear in the phonon energy region 130–180  $\text{cm}^{-1}$  and no combinations or overtones of these are observed. Also, a relatively small number of vibronics is observed for a complicated 24 branch phonon spectrum. All these rule out the possibility for multiphonon lines. The fact that the lines are polarized rules out the possibility of a combination of an acoustical phonon and an optical phonon.

For most vibronic lines it is impossible to make a unique assignment and a set of equivalent assignments

<sup>15</sup> F. Varsanyi, Bull. Am. Phys. Soc. **10**, 609 (1965).

is given (Table VI). All the possible assigned branches give rise to the same set of vibronic selection rules. Obviously, a vibronic line which arises from a single point in the B.Z. is too weak to be detected. The detectable lines are due to a large number of phonons having very close energies. The strong polarization of the lines indicate that all these phonons have the same symmetry with respect to the RE ion site group. Therefore, the vibronic lines are due to portions of phonon branches having  $\mathbf{k}$ 's along directions of high symmetry in the B.Z. For this reason all the assignments of Table VI consist of a direction of high symmetry, e.g.  $T$ ,  $\Delta$ ,  $P$ , etc. The addition of a point of high symmetry (e.g.  $T_1+K_1$ ) suggests that the phonon branch might be flat along a direction which terminates at this point, giving rise to a compatible set of vibronic selection rules. This result is consistent with observations of phonon branches in other crystals by means of neutron diffraction. These studies reveal that flat regions of  $\omega(\mathbf{k})$  are obtained for large intervals of  $\mathbf{k}$  along directions of high symmetry in the B.Z. Flat regions occur also for  $\mathbf{k}$ 's for which the factor group of the group of  $\mathbf{k}$  contains the identity only. These phonons will give rise to unpolarized vibronic bands. The data obtained here (cf. Figs. 1 and 3) indicates that a substantial part of the vibronic spectrum probably arises from such regions in the B.Z. The corresponding vibronic transitions give rise to the strong broad bands on which the polarized peaks are superimposed.

Vibronic transitions due to phonons with energies of the  $\mathbf{k}=0$  Raman and infrared active modes are observed in the spectra. The Raman spectrum was obtained by Hougén and Singh<sup>16</sup> and the infrared spectrum by Varsanyi, Berreman, and Unterwald.<sup>17</sup> In these cases one knows the phonon branch at  $\mathbf{k}=0$  and the vibronic spectra enables one to determine the flat part of the branch for  $\mathbf{k}\neq 0$ . For example, the  $\Gamma_{2,3}^+$  ( $E_{2g}$ ) Raman active modes of  $\text{NdCl}_3$  have phonon energies of 104, 217, and 223  $\text{cm}^{-1}$ . The vibronic lines corresponding to these phonon energies indicate that the branches involved are  $\Delta_3$ ,  $T_1$ , and  $T_1$ , respectively.

Of some interest are the phonons with energies of 72, 78, and 83  $\text{cm}^{-1}$ . They appear on the edge of the broad-band absorption due to the acoustical phonons. They may be due to flat portions of the acoustical branches close to the surface of the B.Z. The phonon branch with energy of 72  $\text{cm}^{-1}$  has the possible assignments  $P_1$  or  $\Delta_1$  or  $\Delta_2$ . From the compatibility relations (Table IV) it is seen that the acoustic branch  $\Gamma_1^- (=A_u)$ , with vibrations in the  $z$  direction at  $\mathbf{k}\approx 0$  is compatible with  $\Delta_1$ . The phonon branch with energy of 78  $\text{cm}^{-1}$  is assigned to a  $T_1+K_{2,3}$  type. Equivalent assignments are  $T_1'+K_{2,3}'$ ,  $S_1+H_{2,3}$ , and  $S_1'+H_{2,3}'$ . The acoustic branch  $\Gamma_{5,6}^- (=E_{1u})$ , vibrations in the  $xy$  plane at  $\mathbf{k}\approx 0$  is compatible with  $T_1$ . Finally, for the phonon

TABLE VI. Vibrational levels of  $\text{NdCl}_3$ .

$\bar{\nu}$ $\text{cm}^{-1}$	Assignment
72	$\Delta_1$ or $\Delta_2$ or $P_1$
78	$T_1+K_{2,3}$
83	$T_1+K_{2,3}$ or $T_1+K_1$ or $\Sigma_1+M_1$ or $\Sigma_1+M_3$
92	$\Delta_1+A_1$ or $\Delta_2+A_1$
98	$\Delta_1+A_1$ or $\Delta_2+A_1$
104	$\Delta_3+\Gamma_{2,3}^+$
110	$\Delta_1+A_1$ or $\Delta_2+A_1$
120	$\Delta_1$ or $\Delta_2$ or $P_1$
124	$\Sigma_1+M_1$ or $\Sigma_1+M_3$ or $T_1+K_1$ or $T_1+K_{2,3}$
129	$\Delta_3$ or $\Delta_6$ or $L_1$ or $U_1$ or $U_2$
134	$P_{2,3}+K_{2,3}$
139	$T_1+K_1$ or $T_1+\Gamma_4^-$
154	$\Sigma_1+M_1$ or $\Sigma_1+M_3$ or $T_1+K_1$ or $T_1+K_{2,3}$
156	$T_2+\Gamma_{2,3}^-$ or $T_2+K_{5,\ell}$
159	$\Delta_1+A_1$ or $\Delta_2+A_1$
161	$\Sigma_2+M_2$ or $\Sigma_2+M_4$ or $T_2+K_4$ or $T_2+K_{5,6}$
163	$\Delta_5+\Gamma_{5,6}^-$ or $\Delta_6+\Gamma_{5,6}^-$
167	$T_2+\Gamma_1^-$ or $T_2+K_4$
170	$\Delta_4+A_3$ or $\Delta_5+A_3$
173	$T_1+\Gamma_4^-$ or $K_1+P_1$
181	$T_1+\Gamma_1^+$
187	$\Delta_1+A_1$ or $\Delta_2+A_1$
192	$\Delta_5+\Gamma_{5,6}^+$ or $\Delta_6+\Gamma_{5,6}^+$
196	$\Delta_5+\Gamma_{5,6}^-$
201	$\Delta_6+\Gamma_{5,6}^-$
217	$T_1+\Gamma_{2,3}^+$
223	$T_1+\Gamma_{2,3}^+$
227	$T_1+K_{2,3}$
234	$\Delta_1+A_1$ or $\Delta_2+A_1$
239	$\Delta_1$ or $\Delta_2$
254	$\Delta_6+\Gamma_{5,6}^-$ or $\Delta_2+\Gamma_1^-$
259	$T_1+\Gamma_{5,6}^-$ or $T_1+K_{2,3}$

branch with energy of 83  $\text{cm}^{-1}$  the possible assignments are  $T_1+K_{2,3}$  or  $T_1+K_1$  or  $\Sigma_1+M_1$  or  $\Sigma_1+M_3$ .  $\Gamma_{5,6}^-$  is compatible with either  $T_1$  or  $\Sigma_1$ . Thus, these branches may be parts of the acoustical branches.

Vibronic transitions due to a given phonon branch were observed accompanying 10 different electronic transitions of both  $\text{Pr}^{3+}$  and  $\text{Nd}^{3+}$ . As explained in III, the phonon energies are independent of the electronic states in which the ions can be found. The fact that the vibronic states associated with various electronic states differ slightly in their separations from their parents is due to the energy correction  $\delta$  of Eq. (10). From the data we estimate the upper limit on  $\delta$  to be 1  $\text{cm}^{-1}$  for both  $\text{Pr}^{3+}$  and  $\text{Nd}^{3+}$ .

## VI. CONCLUSION

It is shown that the polarized vibronic spectra of RE ion in crystals and their Zeeman effect provide information on the phonon spectrum of the crystal. A comparison between the vibrational frequencies derived from the  $\text{Pr}^{3+}$  spectrum and those obtained from the  $\text{Nd}^{3+}$  spectrum shows that the impurity ions interact with the host lattice vibrations. Localized modes are, therefore, unimportant in the case in which a RE ion substitutes another RE ion which is a normal constituent of the crystal. The energy correction to the vibronic and electronic states due to  $V_{ev}$  is small enough, so that the vibrational frequencies derived

<sup>16</sup> J. T. Hougén and S. Singh, Proc. Roy. Soc. (London) A277, 193 (1964).

<sup>17</sup> F. Varsanyi (private communication).

from the vibronic transitions correspond to host-lattice vibrations. The analysis of vibronic transitions of trivalent RE ions is complementary to the conventional methods of studying phonons spectra, namely neutron diffraction, Raman and infrared spectroscopy. Although the vibronic spectrum reflects the structure of  $g(\omega)$ , an unambiguous assignment of the peaks of this function to phonon branches can only be done for crystals with

a small number of branches. Nevertheless, the set of equivalent assignments, obtained in this study, is of use for studies in which a single RE ion is considered, as for example, phonon-induced relaxation. This is because in the reduction of the space-group representations into those of the RE-ion site symmetry group, equivalent assignments give rise to the same reduction, i.e., the same sum of representations.

PHYSICAL REVIEW

VOLUME 161, NUMBER 2

10 SEPTEMBER 1967

## Vibronic Transitions of Hexagonal Rare-Earth Trichlorides. II. Pr<sup>3+</sup> in LaCl<sub>3</sub>, PrCl<sub>3</sub>, and GdCl<sub>3</sub>\*†

ELISHA COHEN AND H. W. MOOS†

*Department of Physics, The Johns Hopkins University, Baltimore, Maryland*

(Received 12 April 1967)

The absorption spectra of Pr<sup>3+</sup> in LaCl<sub>3</sub>, PrCl<sub>3</sub>, and GdCl<sub>3</sub> have been obtained under high resolution in the region 4300–4900 Å. Strong vibronic transitions are observed accompanying the transitions from <sup>3</sup>H<sub>4</sub> ( $\mu = \pm 2$ ) to all components of the groups <sup>3</sup>P<sub>0,1,2</sub>. The correspondence between the vibronic transitions and their parent electronic transitions is made by comparing the splittings in a magnetic field parallel to the crystal *c* axis. Assuming a model of a single Pr<sup>3+</sup> ion interacting with the lattice vibrations, electric dipole selection rules are derived for the case of an applied magnetic field. Using these selection rules, possible assignments of phonon branches are given to the observed vibrational levels. The shifts in phonon frequencies as one goes from LaCl<sub>3</sub> to GdCl<sub>3</sub> are found to be larger for branches which are flat near  $\mathbf{k}=0$  than for those which are flat closer to the edge of the Brillouin zone.

### I. INTRODUCTION

IN the previous paper,<sup>1</sup> the vibronic spectrum of Pr<sup>3+</sup> in NdCl<sub>3</sub> was compared with the vibronic spectrum of Nd<sup>3+</sup> itself. It was demonstrated that the Pr<sup>3+</sup> vibronics are due to phonons of the host lattice. Therefore, Pr<sup>3+</sup> can be used to probe the phonon spectra of other rare-earth (RE) crystals. Pr<sup>3+</sup> is particularly suitable for such studies as it shows strong vibronics (relative to other RE ions) accompanying Stark manifolds with a small number of components ( $J \leq 2$ ). The large differences between the parallel Zeeman splitting factors of the various Stark components of a given group make it possible to associate a given vibronic state with one of these components. In this study, the vibronic transitions of Pr<sup>3+</sup> in three isostructural RECl<sub>3</sub> crystals were studied. La, Pr, and GdCl<sub>3</sub> belong to the space group  $C_{6h}^2(P6_3/m)$ . All of these are often used as host crystals for other RE ions and a knowledge of the phonon spectrum of them is desirable. Previous studies

of the vibronic transitions of Pr<sup>3+</sup> in LaCl<sub>3</sub> and LaBr<sub>3</sub> were done by Satten and his collaborators.<sup>2,3</sup>

The analysis of the experimental data is done along the lines described in detail in Ref. 1. The purpose is to assign phonon branches to the observed vibrational levels. The polarization behavior of the vibronic transitions indicates that the sharp peaks are due to optical phonon branches which are flat along directions of high symmetry in the Brillouin zone (B.Z.).

### II. EXPERIMENTAL RESULTS

The experimental techniques used in this study were described in Ref. 1. All the crystals used in this work were grown and encapsulated in quartz tubing by E. F. Williams of this laboratory. The LaCl<sub>3</sub> and GdCl<sub>3</sub> crystals contained 1% Pr, nominally. The samples which were used to obtain the absorption vibronic transitions were 3 mm thick. The electronic transitions of Pr<sup>3+</sup> in GdCl<sub>3</sub> were obtained from a 0.5-mm thickness crystal. The thinnest PrCl<sub>3</sub> sample available was 0.2 mm thick. Even with such a crystal, the vibronic transitions accompanying the transitions from the ground state (<sup>3</sup>H<sub>4</sub>,  $\mu = \pm 2$ ) to the excited states <sup>3</sup>P<sub>1</sub> and <sup>3</sup>P<sub>2</sub> were highly overabsorbed and showed a band

\* Partially supported by the National Aeronautical and Space Administration under Grant No. NsG-361.

† Based in part on a Ph.D. dissertation by E. Cohen, The Johns Hopkins University, 1967 (unpublished). Available through University Microfilms, Ann Arbor, Michigan.

‡ Alfred P. Sloan Foundation Fellow.

<sup>1</sup> Elisha Cohen and H. W. Moos, preceding paper, Phys. Rev. **161**, 258 (1967).

<sup>2</sup> I. Richman, R. A. Satten, and E. Y. Wong, J. Chem. Phys. **39**, 1833 (1963).

<sup>3</sup> R. A. Satten, J. Chem. Phys. **40**, 1200 (1964).